

Hydrodynamics of superfluids confined in blocked rings and wedges

Chandan Dasgupta*

*Centre for Condensed Matter Theory, Department of Physics,
Indian Institute of Science, Bangalore 560012, India*

Oriol T. Valls†

School of Physics and Astronomy, University of Minnesota, Minneapolis, Minnesota 55455

(Dated: June 16, 2008)

Motivated by the many recent experimental studies of non-classical rotational inertia (NCRI) in superfluid and supersolid samples, we present here a study of the hydrodynamics of a superfluid confined in the two-dimensional region (equivalent to a long cylinder) between two concentric arcs subtending an angle β , with $0 \leq \beta \leq 2\pi$. The case $\beta = 2\pi$ corresponds to a blocked ring. We discuss the methodology to compute the NCRI effects, and calculate these effects both for small angular velocities, when no vortices are present, and in the presence of a vortex. We find that, for a blocked ring, the NCRI effect is small, and that therefore there will be a large discontinuity in the moment of inertia associated with blocking or unblocking circular paths. A number of mathematical issues are pointed out and resolved.

PACS numbers: 47.37.+q, 47.32.Ef

I. INTRODUCTION

Flow without dissipation is the defining feature of superfluidity. Because of this property the moment of inertia of a vessel containing a superfluid is different from (smaller than) that when the liquid is in the normal state. This effect is largest in the absence of vortices, when superfluid flow is irrotational. The difference between the moments of inertia when the liquid, confined by boundary conditions, is in the normal and superfluid states is known as the “non-classical rotational inertia” (NCRI). The occurrence of NCRI is often used as an experimental signature of superfluidity. Superfluid hydrodynamics and the resulting NCRI have been studied extensively [1] in the past for simple geometries, such as spherical, cylindrical or rectangular containers rotating about a symmetry axis. Because of several recent developments, some of which are briefly discussed below, it has become necessary to understand the properties of flow of superfluids in enclosures of more complicated geometry. These provide the motivation for our present study.

Recent observations [2–6] of NCRI in torsional oscillation experiments on solid ^4He have been interpreted as the occurrence of a “supersolid” phase. This interpretation of the experimental results is controversial. There is experimental [5, 7] and theoretical [8] evidence suggesting that the observed NCRI is due to superfluidity along grain boundaries in a polycrystalline sample. Since the grain boundaries in polycrystalline samples form com-

plex disordered structures, calculations of the flow properties and the rotational inertia of a superfluid confined in irregular-shaped channels are necessary for a quantitative assessment of whether this mechanism is the correct explanation of the observed results. In this context, it is important to examine whether the superfluid component can flow along continuous closed paths in the sample. Since the geometry of the network of grain boundaries would depend on thermodynamic variables such as the temperature and pressure, and on the cell geometry, the availability of such paths would also depend on these parameters and conditions. Thus, an understanding of the dependence of the NCRI on such variables requires, for example, a calculation of how the NCRI arising from a blocked ring of superfluid changes as the blockage is removed. To check whether the observed NCRI is due to the occurrence of superfluidity, the NCRI of samples in which the solid ^4He is confined in the annular region between two concentric cylinders has been measured [2] in the presence of a barrier in the annulus that prevents possible flow of the superfluid along a closed path surrounding the rotation axis (the common axis of the cylinders). The NCRI observed under these conditions is found to be much smaller than that for samples in which the artificial block is not present. The calculation just mentioned is obviously relevant for a quantitative understanding of the results of such experiments. Finally, an understanding of experimental results [6] on the dependence of the NCRI on the frequency of torsional oscillations requires a theoretical understanding of vortex formation and critical velocity in superfluids confined in irregular-shaped channels.

The recent explosion of activity in experimental and theoretical studies of superfluidity and other quantum phenomena in trapped, ultracold atomic systems provides another motivation for our study. Various signatures of superfluidity, such as persistent flow, NCRI and

*Electronic address: cdgupta@physics.iisc.ernet.in; Also at Condensed Matter Theory Unit, Jawaharlal Nehru Centre for Advanced Scientific Research, Bangalore 560064, India

†Electronic address: otvalls@umn.edu; Also at Minnesota Supercomputer Institute, University of Minnesota, Minneapolis, Minnesota 55455

formation of quantized vortices have been observed in both bosonic [9–11] and fermionic [12] systems. While the early experiments on such systems were carried out for traps with simple geometry, more recent experiments have begun to explore the properties of superfluid condensates in traps with more complex structure. Superfluid flow in a toroidal trap has been observed recently [11], and experimental conditions under which a ring-shaped optical trap can be realized have been suggested [13]. Studies of superfluid hydrodynamics in containers with complex geometry are obviously relevant for understanding the results of experiments on superfluidity in atomic systems confined in such traps.

A third and also important motivation is that there have been many experimental studies of the flow properties and NCRI of superfluids confined in porous media such as vycor glass and containers packed with fine powder [14, 15]. The first experimental observation [16] of “supersolid” behavior was for solid ^4He confined in vycor glass. Since the pores in these systems have complex geometry, it is necessary to work out the hydrodynamics of superfluids in irregular-shaped channels in order to understand the results of these experiments in quantitative detail.

To shed light on the flow properties of confined superfluids, we have studied the hydrodynamics of a superfluid confined in a two-dimensional region between two concentric circular arcs, each of which subtends an angle β at their common center. The annular region between the two arcs is bounded on two sides by straight walls along the radial direction. Thus, the special case with $\beta = 2\pi$ corresponds to a ring that is blocked by a wall placed perpendicular to its inner and outer peripheries. This two-dimensional geometry corresponds, neglecting edge effects, to that used in many experiments on supersolid behavior in ^4He where the helium is confined in the annular region between two concentric cylinders, under the assumption that the cylinders are long enough and the confined system is homogeneous along the cylinder axis. In the limit of vanishing inner radius, this geometry corresponds to that of a wedge with opening angle β . The limit $\beta = 2\pi$ in this case represents a circular container with a straight blocking wall extending from the center of the circle to its periphery.

We assume throughout the paper that the fluid is incompressible. We first consider the case where there are no vortices (so that the superfluid flow is irrotational), and solve the hydrodynamic equation for the velocity field for rotation about an axis perpendicular to the plane of the system and passing through the common center of the arcs that form its boundary. The sample geometry is reflected in the boundary conditions for the velocity field. For incompressible and irrotational flow, the velocity field can be expressed in terms of either a scalar or a vector potential (stream function), analogous to those in electromagnetic theory, both of which satisfy the Laplace equation with appropriate boundary conditions. The scalar potential method is simpler, and leads to series that con-

verge rapidly. We have used this method to obtain the velocity field for $\beta = 2\pi$ and $\beta = \pi$. For a general value of β , however, the stream function method, although more difficult in that it leads to series that are not convergent, but Borel summable, is more powerful. We have therefore used it to obtain the velocity field for arbitrary β . We present analytic results for the velocity field and the moment of inertia for arbitrary values of the inner and outer radii and the opening angle β . We also derive a simple “parallel axis” theorem that relates the moment of inertia for rotation about any axis perpendicular to the plane of the system to the calculated value for rotation about an axis passing through the center of mass.

In the context of experimental observations of NCRI in solid ^4He , the most important result of our study is about the NCRI of a blocked ring. When the ring is blocked, the superfluid can not flow through it. However, due to the irrotational nature of superfluid flow, the moment of inertia is smaller than that for rigid-body rotation. Therefore, the drop in the moment of inertia when the block is removed (the superfluid does not contribute to the moment of inertia when there is no block) is less than the rigid-body value. Our calculations show that the moment of inertia of a blocked ring whose width is small compared to its radius is very close to its moment of inertia for rigid rotation, so that unblocking the ring (i.e. the opening up of a closed path) produces a large drop in the moment of inertia (nearly equal to its rigid-rotation value), which would show up in an experiment as a relatively large value of the NCRI.

Our calculations uncover several interesting mathematical issues and we indicate ways of addressing them. Some of these were also present in earlier studies [1] of superfluid hydrodynamics, while some are new. We discuss these questions as they appear throughout the paper. We consider also the nucleation of vortices in the sample. As pointed out in Ref. [1], states with vortices present will have, at sufficiently larger values of the angular velocity Ω , a lower free energy than the vortex-free state. One new result is that the velocity field for a wedge with $\beta > \pi$ formally diverges at the tip of the wedge for *any* nonzero value of Ω . This means that the implicit assumption that the velocity field nowhere exceeds the critical velocity is in principle mathematically incorrect for these wedges: for any nonzero value of Ω , there must be a region near the tip where the liquid is in the normal state. Although in practice, as we will see, the size of the region where this occurs is too small to have any measurable consequence in the usual geometries, it may be an important point in other cases. We show that this divergence of the velocity can be removed by the presence of a single vortex. We calculate the position of this vortex and the rotational inertia in its presence. This result suggests that vortices may be present in these systems even if the angular speed of rotation is arbitrarily small, implying that the critical angular speed for the nucleation of a vortex is zero. Whether this happens or not would be determined by a balance between the free-energy cost

of creating a vortex and that of creating a normal region near the tip. We will show that in typical experimental situations, the free energy cost of creating a vortex is the relevant one and vortices do not occur for sufficiently small angular velocities. We calculate the critical angular velocity for vortex nucleation, which turns out, for typical samples, to be in the experimentally important range of angular velocities. We show how the rotational inertia is modified by these vortex excitations.

The rest of this paper is organized as follows. In section II, we describe in detail our calculations. We present first two alternative methods of calculating the velocity field in the vortex free case, and discuss the results obtained for this field and the moment of inertia. We then explain how to include the nucleated vortices. A summary of our results and a discussion of their implications for experimental studies of superfluidity are presented in the concluding section III.

II. RESULTS

A. Formulation of the problem

We consider, as explained above, superfluid flow in an ideal cylinder, long enough in the z direction so that edge effects are negligible and the problem quasi two-dimensional. The cross sections of the cylinders that we will consider will be bounded by two concentric circular arcs of radii a and b (with $a > b$) and encompassing an angle that we will call β . In the limit $b = 0$ the shape of this cross section is that of a circular wedge. We will consider all values of β , $0 < \beta \leq 2\pi$. It must be emphasized that the case $\beta = 2\pi$ is not the same as that of a ring, since a boundary along a radius still exists.

In the absence of vortices (the generalization to the case when vortices are present will be discussed below) the superfluid velocity field $\mathbf{v}(\mathbf{r})$ for an incompressible fluid satisfies the equations:

$$\nabla \cdot \mathbf{v}(\mathbf{r}) = 0 \quad (2.1a)$$

$$\nabla \times \mathbf{v}(\mathbf{r}) = 0. \quad (2.1b)$$

The boundary condition, corresponding to rotation around some center O with uniform angular velocity $\boldsymbol{\Omega}$ is:

$$\mathbf{v}(\mathbf{r})_{\perp} = (\boldsymbol{\Omega} \times \mathbf{r})_{\perp} \quad (2.2)$$

where \mathbf{r} is a vector from O to a point on the boundary, and the index \perp denotes the component perpendicular to the boundary. The point O is not necessarily the center of mass of the system: in general we will take it to be, for reasons of obvious computational convenience, the center of the arc or arcs that are part of the boundaries of our system.

There are two obvious ways to solve Eqs. (2.1). The first is to introduce a scalar potential $V(\mathbf{r})$ such that

$\mathbf{v}(\mathbf{r}) = \nabla V(\mathbf{r})$. In that case $V(\mathbf{r})$ satisfies the Laplace equation:

$$\nabla^2 V(\mathbf{r}) = 0 \quad (2.3)$$

and Eq. (2.2) is a Neumann boundary condition on V . Alternatively, one can introduce a stream function $\Psi(\mathbf{r})$ such that:

$$v_x = -\partial\Psi/\partial y \quad (2.4a)$$

$$v_y = \partial\Psi/\partial x, \quad (2.4b)$$

where one can think of Ψ as the z component of a vector potential [$\mathbf{v}(\mathbf{r}) = -\nabla \times (\hat{z}\Psi(\mathbf{r}))$]. It is obvious that $\Psi(\mathbf{r})$ satisfies the Laplace equation:

$$\nabla^2 \Psi(\mathbf{r}) = 0 \quad (2.5)$$

Now, however, the boundary conditions are of the Dirichlet form [1]: at any point in the boundary,

$$\Psi(\mathbf{r}) = \frac{1}{2}\Omega r^2. \quad (2.6)$$

It turns out, as we will see, that for certain special values of β such as π and 2π , the scalar potential method is much simpler to use and leads to expressions for $\mathbf{v}(\mathbf{r})$ in the form of rapidly convergent series which are very convenient. However, for other values of β , this method becomes rather awkward. The stream function method on the other hand can be used for any value of β , but the resulting expressions involve asymptotic series. These are, however, Borel summable and agree with the results obtained from $V(\mathbf{r})$ in the cases where the scalar potential method works well. For this reason, we will first present here results obtained from $V(\mathbf{r})$ for $\beta = 2\pi$ and $\beta = \pi$ and then consider the general case using the stream function.

Once the velocity field is obtained, the angular momentum (and hence the moment of inertia) can be calculated by straightforward integration of the velocity field. In this way, the depletion of the moment of inertia from its rigid body value is obtained. In general our origin O is not the center of mass (COM) of the system: therefore it is important to discuss an interesting property of the nature of the parallel axis theorem shift in the superfluid case. If one considers the moment of inertia of the superfluid with respect to the COM, I_{SF}^{COM} one finds, of course, that it is always smaller than that of the corresponding rigid object (RO) of the same shape and density, I_{RO}^{COM} . Indeed, for the case of a circle I_{SF}^{COM} vanishes. With respect to an arbitrary origin O one has for the superfluid a total moment of inertia $I_{SF}^T = I_{SF}^{COM} + I_{SF}^{PA}$ where the last term is the parallel axis shift. The key point here is that this shift is the same as that for the rigid object. One has:

$$I_{SF}^{PA} = I_{RO}^{PA}. \quad (2.7)$$

The proof of this theorem is very simple: the problem, as defined by the above equations and boundary conditions, is linear. If one shifts the origin from the COM to

a point a distance \mathbf{R} away from it, the velocity field of the boundaries shifts to $\mathbf{v} = (\mathbf{r} + \mathbf{R}) \times \boldsymbol{\Omega}$. In view of this, the linearity of the problem, and the boundary condition Eq. (2.2), the solution of the shifted problem is the velocity field computed with respect to rotations around the COM, plus a uniform velocity field $\mathbf{R} \times \boldsymbol{\Omega}$. This second field trivially satisfies the equations and takes care of the additional term in the boundary condition. But it is trivial to verify that such a constant field leads simply to a parallel axis theorem shift in the moment of inertia equal to that for the corresponding rigid object. This applies irrespective of the shape of the object: it is not limited to the wedge shapes considered here. It is straightforward to check by direct calculation that it applies, for example, to the ellipsoidal shapes of Ref. 1. This theorem has physical consequences: since the parallel axis shift cannot be “depleted” from its RO value by the superfluid flow, in general the fractional depletion of I_{SF} will always be largest when the rotation is around the COM.

B. Scalar potential method for $\beta = 2\pi$ and $\beta = \pi$

To illustrate the results, let us first turn to the simplest case where $\beta = 2\pi$, $b = 0$ (a circle with a wall along its radius). For this case, one can very simply use the scalar potential method. We write, in polar coordinates:

$$V(r, \phi) = \sum_{m \geq 1} a_m r^{m/2} \sin(m\phi/2) + \sum_{m \geq 1} b_m r^{m/2} \cos(m\phi/2). \quad (2.8)$$

With the radial wall set along the $\phi = 0$ direction, the azimuthal component of the velocity,

$$v_\phi(r, \phi) = \sum_{m \geq 1} \frac{m}{2} a_m r^{m/2-1} \cos(m\phi/2) - \sum_{m \geq 1} \frac{m}{2} b_m r^{m/2-1} \sin(m\phi/2) \quad (2.9)$$

must equal Ωr at $\phi = 0$. This immediately tells us that all the a_m vanish except a_4 , which equals $\Omega/2$. The radial component is then:

$$v_r(r, \phi) = \Omega r \sin(2\phi) + \sum_{m \geq 1} \frac{m}{2} b_m r^{m/2-1} \cos(m\phi/2) \quad (2.10)$$

At $r = a$ we have $v_r = 0$ and hence:

$$-\Omega a \sin(2\phi) = \sum_{m \geq 1} \frac{m}{2} b_m a^{m/2-1} \cos(m\phi/2) \quad (2.11)$$

from which one obtains that all the b_n with even n are zero while for odd n :

$$b_n = \frac{32\Omega a}{\pi n(n^2 - 16)a^{n/2-1}}. \quad (2.12)$$

From these and Eqs. (2.9) and (2.10) we have the final result for the velocity field:

$$v_r(r, \phi) = \Omega r \sin(2\phi) + \frac{16\Omega a}{\pi} \sum_{n \text{ odd}} \rho^{n/2-1} \frac{1}{n^2 - 16} \cos(n\phi/2) \quad (2.13a)$$

$$v_\phi(r, \phi) = \Omega r \cos(2\phi) - \frac{16\Omega a}{\pi} \sum_{n \text{ odd}} \rho^{n/2-1} \frac{1}{n^2 - 16} \sin(n\phi/2) \quad (2.13b)$$

where $\rho \equiv r/a$.

Two remarks are needed about these simple results; first, the series involved are very rapidly convergent. Second, the velocity components have a square root singularity at the origin. Physically, this is not important: the relevant number is the value of r at which the velocity would exceed the Landau critical velocity[17] $v_c \approx 2.5 \times 10^4 \text{ cm/s}$. For typical experimental situations, the maximum value of Ω is less than 0.1 s^{-1} (see for example[2, 6]). This would mean that only at values of r/a around 10^{-11} would v_c be exceeded. Such small values of r would not have any experimentally measurable consequence (the hydrodynamic description we use would not even apply to such length scales). Also this divergence is not present for nonzero values of the inner

radius b , and the inner radius is finite (of order 10^{-2} cm) in torsion and rotation experiments. Mathematically, the singularity is integrable, and allows for the formal calculation of the moment of inertia. However, the above does mean that the assumption that the velocity is lower than v_c everywhere in the system or that no vortex is present in the system may not be strictly correct in certain geometries. There may be experimentally realizable situations where this effect would have observable consequences. This is discussed in detail in sections IID and IIE.

The angular momentum is obtained by integration of rv_ϕ over the sample and the moment of inertia is just the ratio of the angular momentum and the angular velocity Ω . We will use units in which the areal mass density is

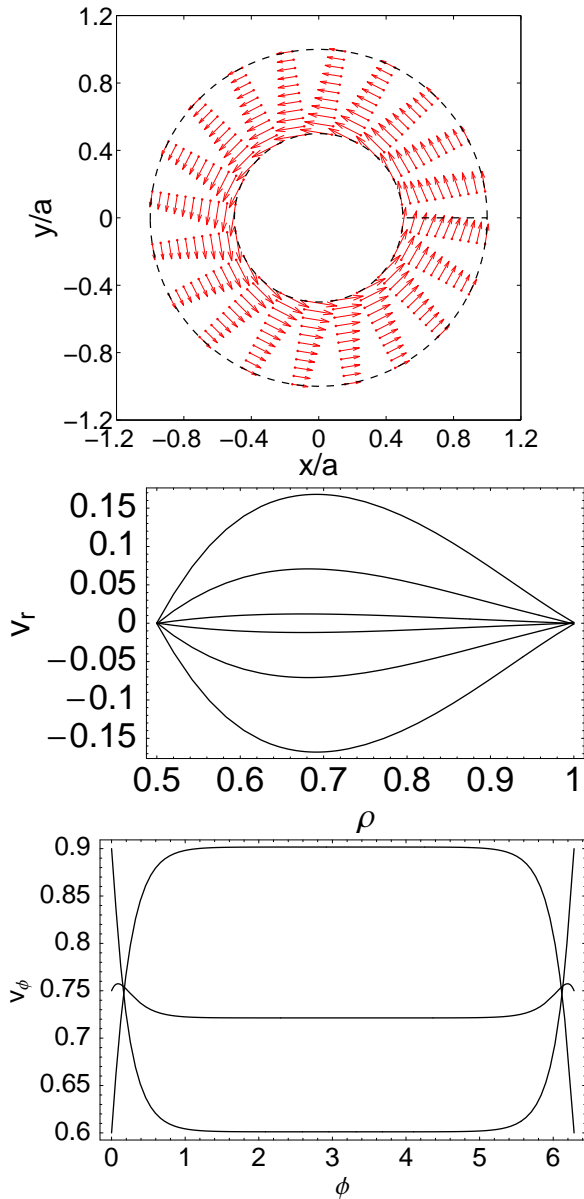


FIG. 1: The velocity field for a blocked ring with $c = 0.5$. The first panel shows the relative strengths of the velocity field as a function of position. The second panel is the radial component (in units of Ωa) plotted vs $\rho \equiv r/a$ at azimuthal angles ϕ (from bottom to top) $\pi/16, \pi/8, \pi/4, 7\pi/4, 15\pi/8, 31\pi/16$. The third panel, in the same units, shows the azimuthal component of the velocity vs. ϕ at $\rho = 0.6, 0.75, 0.9$.

unity. We obtain the result:

$$I_{SF} = -\frac{128a^4}{\pi} \sum_{n \text{ odd}} \frac{1}{n(n^2 - 16)(n + 4)}, \quad (2.14)$$

which, after numerically evaluating the rapidly convergent series, gives $I_{SF} = 0.693a^4$. Thus we have for this

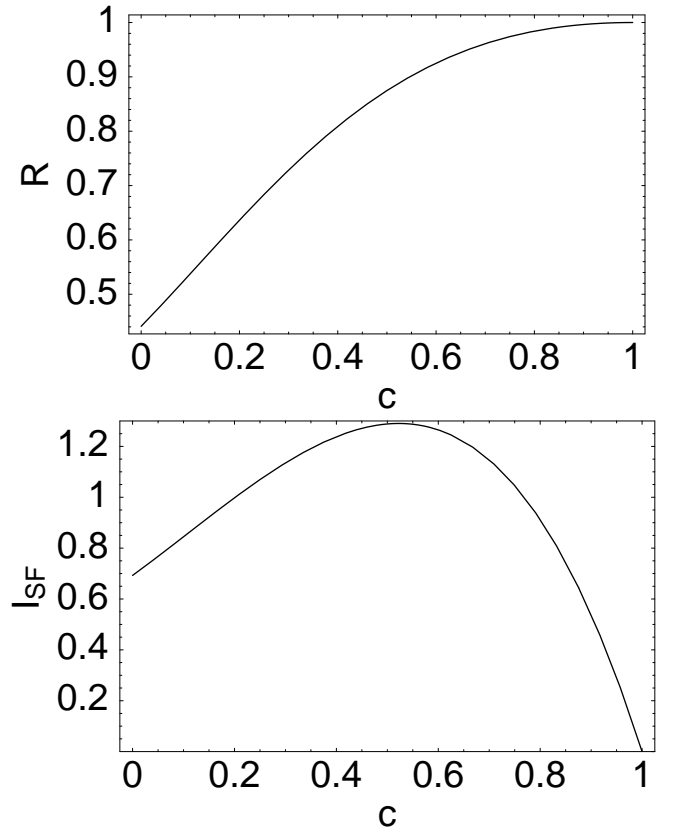


FIG. 2: Moment of inertia of an obstructed ring in terms of its aspect ratio $c \equiv b/a$. In the top panel the ratio R of I_{SF} (Eq. (2.22)) to the rigid body value is plotted, while in the bottom panel we plot I_{SF} itself, in units such that $a = 1$. The maxima in the two plots are at different values of c .

obstructed circle:

$$\frac{I_{SF}}{I_{RO}} \approx 0.441. \quad (2.15)$$

The same method can be used at $\beta = \pi$. In that case the only significant difference is that in the expression for $V(\mathbf{r})$ one must write:

$$V(r, \phi) = \sum_{m \geq 1} a_m r^m \sin(m\phi) + \sum_{m \geq 1} b_m r^m \cos(m\phi). \quad (2.16)$$

As before, all the coefficients a_n are determined from the boundary conditions on v_ϕ at $\phi = 0$ and $\phi = \pi$. Both are satisfied if all a_n vanish except $a_1 = \Omega/2$. The b_n are determined then from the boundary condition on v_r . The result for the velocity field is:

$$v_r(r, \phi) = \Omega r \sin(2\phi) + \frac{8\Omega a}{\pi} \sum_{n \text{ odd}} \rho^{n-1} \frac{1}{n^2 - 4} \cos(n\phi) \quad (2.17a)$$

$$v_\phi(r, \phi) = \Omega r \cos(2\phi) - \frac{8\Omega a}{\pi} \sum_{n \text{ odd}} \rho^{n-1} \frac{1}{n^2 - 4} \sin(n\phi). \quad (2.17b)$$

The series are again convergent, and now the previously found integrable singularity at the origin is absent. The moment of inertia with respect to the origin is:

$$I_{SF} = -\frac{16a^4}{\pi} \sum_{n \text{ odd}} \frac{1}{n(n^2 - 4)(n + 2)}. \quad (2.18)$$

Numerically, we have $I_{SF} = 0.488a^4$ which gives a ratio $I_{SF}/I_{RO} = 0.621$, a value higher than that for the circle. However, we must recall that in this case O is not the COM and that (as shown above) there is no reduction in the parallel axis term so that from the point of view of the COM the reduction must be larger. Indeed one finds that:

$$\frac{I_{SF}^{COM}}{I_{RO}^{COM}} = 0.41, \quad (2.19)$$

which is actually a little less than that for the circle.

One can see that it is awkward to extend this simple procedure to other values of β . If one sets for example $\beta = \pi/2$ and doubles again the angles and powers in the expression for $V(\mathbf{r})$ one finds that it is not possible

to satisfy the boundary condition for v_ϕ at $\phi = 0$ and $\phi = \pi/2$ from a single term in the first sum (the a_n coefficients) in the potential. Similar difficulties are found at e.g. $\beta = 3\pi/2$. Although these difficulties should not be unsurmountable, we will instead use the stream function method in the general case and deal appropriately there with the mathematical difficulties associated with the asymptotic series that then result.

However, one can easily generalize this simple procedure, for the above values of β , to the physically more relevant case where $b > 0$. We will consider here the important case of an obstructed ring, $\beta = 2\pi$. In that case one simply has to add to the potential in Eq. (2.8) the appropriate negative powers of r . Taking into account directly the boundary condition on v_ϕ we write:

$$V(r, \phi) = \Omega r \sin(2\phi) + \sum_{m \geq 1} \left(b_m r^{m/2} + \frac{c_m}{r^{m/2}} \right) \cos(m\phi/2). \quad (2.20)$$

The coefficients b_m and c_m are then found from the boundary conditions on v_r at $r = a$ and $r = b$. One then obtains the velocity fields:

$$v_r(r, \phi) = \Omega a \rho \sin(2\phi) \frac{16\Omega a}{\pi} \sum_{n \text{ odd}} \cos(n\phi/2) \frac{1}{(1 - c^n)(n^2 - 16)} \left[\rho^{n/2-1} f_n(c) - \frac{g_n(c)}{\rho^{n/2+1}} \right], \quad (2.21a)$$

$$v_\phi(r, \phi) = \Omega a \rho \cos 2\phi \frac{16\Omega a}{\pi} \sum_{n \text{ odd}} \sin(n\phi/2) \frac{1}{(1 - c^n)(n^2 - 16)} \left[\rho^{n/2-1} f_n(c) + \frac{g_n(c)}{\rho^{n/2+1}} \right]. \quad (2.21b)$$

where $c \equiv b/a < 1$, $f_n(c) = 1 - c^{n/2+2}$ and $g_n(c) = c^n - c^{n/2+2}$. Plots of the fields given by Eqs. (2.21) are shown in Fig. 1. All the plots in the figure are for $c = 0.5$, a value in the region where, as we shall see below, NCRI effects are found to be largest. In the first panel, the vector field is displayed in two dimensions over the entire sample. The units of velocity are arbitrary, but the overall pattern of the field is then clearly shown. In the second and third panels we show a plot of v_r (in units of Ωa) vs r (in units of a) at several values of the azimuthal angle ϕ and a plot, in the same units, of v_ϕ vs ϕ at several values of r . One can see that the boundary conditions are satisfied.

The moment of inertia of the superfluid blocked ring is:

$$I_{SF} = -\frac{128a^4}{\pi} \sum_{n \text{ odd}} \frac{1}{n(n^2 - 16)(1 - c^n)} \left[\frac{1}{n + 4} f_n^2(c) - \frac{1}{n - 4} g_n^2(c) \right], \quad (2.22)$$

The behavior of this quantity as a function of aspect ratio c is well worth noting. In the first panel of Fig. 2 we plot

the ratio $R \equiv I_{SF}/I_{RO}$ for a blocked ring of aspect ratio

c , vs. c . As noted above, the value for $c = 0$ (blocked circle) would, strictly speaking, have to be corrected, but the range of c affected by this is negligible. The ratio R increases very quickly with c : at $c = 1/2$ it already reaches 0.875 while at $c = 0.75$ it exceeds 97%. We see, therefore, that a narrow superfluid circular channel rotating about its center behaves essentially like a rigid body when it is blocked. Since, when unblocked, its moment of inertia vanishes, we see that in such a channel there will be a sharp discontinuity in I as it is blocked or unblocked. In a sample containing a number of such channels, discontinuities or glitches in I will occur as the channels are blocked or unblocked. As $c \rightarrow 1$, $R \rightarrow 1$ and the unblocking would drop R from one to zero, the maximum amount. One should recall, however, that I vanishes at $c = 1$ for both the superfluid and the rigid body. In an experimental situation one would measure the *difference* in I with the channel blocked and unblocked which is I_{SF} itself. This quantity has a broad maximum centered around $c \approx 0.52$ as one can see in the second panel of Fig. 1. There we plot I_{SF} itself in units such that a is unity. From this plot one can see that the important experimental contribution would come from a range of rings with c values in the region 0.2 through 0.8.

C. Stream function method for arbitrary β

As discussed in section II A, the velocity field can be written in terms of a stream function $\Psi(\mathbf{r})$ that satisfies

the Laplace equation with Dirichlet boundary conditions (see Eqs. (2.4- 2.6)). Following Ref. [1], the general solution for $\Psi(\mathbf{r})$ for arbitrary β can be written as

$$\Psi(\mathbf{r}) = \frac{1}{2}\Omega \int dl' r'^2 \mathbf{n}' \cdot \nabla' G(\mathbf{r}', \mathbf{r}), \quad (2.23)$$

where the line integral $\int dl'$ is over the boundary of the system, \mathbf{n}' is a unit vector along the outward normal to the boundary, and $G(\mathbf{r}, \mathbf{r}')$ is the Green's function for the Laplacian operator, satisfying the equation

$$\nabla^2 G(\mathbf{r}, \mathbf{r}') = \delta(\mathbf{r} - \mathbf{r}'), \quad (2.24)$$

and the boundary conditions

$$G(\mathbf{r}, \mathbf{r}') = 0 \quad (2.25)$$

for all \mathbf{r} on the boundary of the system. Thus, $\Psi(\mathbf{r})$ and hence, the velocity field, can be obtained from Eq. (2.23) once an expression for the Green's function, satisfying Eqs. (2.24) and (2.25) is obtained.

As in section II B, we first consider, for simplicity, the case $b = 0$, which corresponds to a wedge of radius a and opening angle β . The Green's function in this case is easily obtained [18] to be

$$G(r, \phi; r', \phi') = -\frac{1}{\pi} \sum_{n=1}^{\infty} \frac{1}{n} r_{<}^{n\pi/\beta} \left(\frac{1}{r_{>}^{n\pi/\beta}} - \frac{r_{>}^{n\pi/\beta}}{a^{2n\pi/\beta}} \right) \sin(n\pi\phi/\beta) \sin(n\pi\phi'/\beta), \quad (2.26)$$

where $r_{>}$ ($r_{<}$) is the larger (smaller) one of the two radial coordinates r and r' . Using this in Eq. (2.23), we obtain the following expression for the stream function $\Psi(\mathbf{r})$:

$$\Psi_{\Omega}(r, \phi) = \frac{2\Omega a^2}{\pi} \sum_{n \text{ odd}} \sin(n\pi\phi/\beta) \left[\frac{n\pi^2/\beta^2}{n^2\pi^2/\beta^2 - 4} \left(-\left(\frac{r}{a}\right)^{n\pi/\beta} + \frac{r^2}{a^2} \right) + \frac{1}{n} \left(\frac{r}{a}\right)^{n\pi/\beta} \right]. \quad (2.27)$$

The radial and azimuthal components of the velocity field, obtained from $\Psi_{\Omega}(r, \phi)$ through the relations

$$v_r = -\frac{1}{r} \frac{\partial \Psi}{\partial \phi}, \quad v_{\phi} = \frac{\partial \Psi}{\partial r}, \quad (2.28)$$

are given by

$$v_r(r, \phi) = \frac{2\Omega a^2}{\pi r} \sum_{n \text{ odd}} \left(\frac{n\pi}{\beta} \right) \cos(n\pi\phi/\beta) \times \left[\frac{n\pi^2/\beta^2}{n^2\pi^2/\beta^2 - 4} \left(\left(\frac{r}{a}\right)^{n\pi/\beta} - \frac{r^2}{a^2} \right) - \frac{1}{n} \left(\frac{r}{a}\right)^{n\pi/\beta} \right], \quad (2.29a)$$

$$v_{\phi}(r, \phi) = \frac{2\Omega a^2}{\pi} \sum_{n \text{ odd}} \sin(n\pi\phi/\beta) \times \left[\frac{2r}{a^2} \frac{n\pi^2/\beta^2}{n^2\pi^2/\beta^2 - 4} - \frac{n\pi}{\beta r} \left(\frac{r}{a}\right)^{n\pi/\beta} \left(\frac{n\pi^2/\beta^2}{n^2\pi^2/\beta^2 - 4} - \frac{1}{n} \right) \right]. \quad (2.29b)$$

Calculation of the velocity field for $\beta = \pi/2$ requires some

care because the denominators of some of the terms in

Eqs. (2.29) go to zero for $\beta = \pi/2$ and $n = 1$. The numerators also vanish for these values of β and n , so that finite contributions that vary smoothly with β across $\pi/2$ are obtained for the velocity components. Similar behavior is found for $\beta = 3\pi/2$ for which the $n = 3$ term in the denominators in Eqs. (2.29) vanishes. These results also exhibit, for $\beta > \pi$, a singularity $r^{\pi/\beta-1}$ as $r \rightarrow 0$, which can be readily seen from Eqs. (2.29) to arise from the $n = 1$ term in the sum. This is in agreement with what we found from the scalar potential method. As discussed in detail in the previous section, this divergence, although mathematically interesting, is not relevant in realistic physical situations and we will ignore it in this part of our discussion. This singularity is always integrable. Therefore, the angular momentum of the superfluid about the origin (tip of the wedge) is easily calculated for all β using these expressions for the velocity components. The result for the moment of inertia about O is

$$I_{SF} = \frac{2a^4}{\pi} \sum_{n \text{ odd}} \frac{1}{n} \left(\frac{n\pi}{\beta} + 4 \right) \frac{1}{(n\pi/\beta + 2)^2}. \quad (2.30)$$

For the case $\beta = 2\pi$, the moment of inertia about the origin is given by the infinite series

$$I_{SF}(\beta = 2\pi) = \frac{4a^4}{\pi} \sum_{n \text{ odd}} \frac{1}{n} \frac{n+8}{(n+4)^2}. \quad (2.31)$$

This infinite series appears to be different from the one in Eq. (2.14) which was obtained using the scalar potential method. In particular, the series in Eq. (2.31) converges more slowly than the one in Eq. (2.14). However, using the identity

$$\sum_{n \text{ odd}} \frac{1}{(n-4)(n+4)} = 0, \quad (2.32)$$

it can easily be shown that these two expressions for the moment of inertia are mathematically identical. We have also checked that a similar situation applies when the results for the moment of inertia obtained from Eqs. (2.29) for $\beta = \pi$ are compared to those obtained in the preceding section using the scalar potential method.

However, the situation is much more complicated when, instead of comparing the moments of inertia, one compares directly the velocity fields obtained by the two methods. In this case it is not sufficient to add or subtract a series that converges to zero. The reason is that while the series in Eqs. (2.13) converge for all angles ϕ and for any $r \neq 0$, those in Eqs. (2.29) and (2.27) do not. This question is related to other technical difficulties with the result (2.27), and in general with the stream function method, which we will further address below.

The moment of inertia of the wedge for rigid-body rotation about O is $I_{RO} = \beta a^4/4$, and its moment of inertia for rigid-body rotation about its COM is given by $I_{RO}^{COM} = I_{RO} - I_{RO}^{PA}$ with $I_{RO}^{PA} = 8a^4 \sin^2(\beta/2)/(9\beta)$. Using these results and Eq. (2.30), we have calculated the

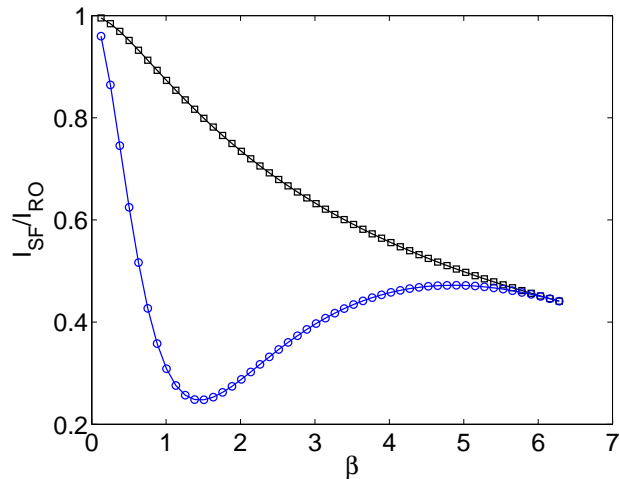


FIG. 3: The ratios I_{SF}/I_{RO} (upper curve), and $I_{SF}^{COM}/I_{RO}^{COM}$ (lower curve) for a superfluid wedge as a function of the opening angle β , $0 < \beta \leq 2\pi$. I_{SF} is calculated from Eq. (2.30).

ratios I_{SF}/I_{RO} and $I_{SF}^{COM}/I_{RO}^{COM}$ as functions of the angle β . The results are shown in Fig. 3. These ratios are of course less than unity, the level of suppression being given by the NCRI effect. In the figure we see that this fractional suppression is always larger in the COM frame, that is, I_{SF}/I_{RO} is always higher than $I_{SF}^{COM}/I_{RO}^{COM}$, except of course at $\beta = 2\pi$ where the two are the same. This is in agreement with the theorem proved at the end of Sec. II A. It is interesting that the ratio $I_{SF}^{COM}/I_{RO}^{COM}$ is not a monotonic function of β – it exhibits a minimum at $\beta = \pi/2$.

A representative plot of the velocity field for a wedge with $\beta = (7/8)2\pi$ is shown in Fig. 4. The velocity vector field is plotted in arbitrary relative units, as in the first panel of Fig. 1. It is instructive to compare that panel with Fig. 4. In the earlier case we have $c = 0.5$ whereas in Fig. 4 we have a wedge, $c = 0$. The rise in the absolute value of the velocity as $r \rightarrow 0$ can now be seen. On the other hand, the behavior of v_r as a function of ϕ is clearly very similar: it follows from the second panel of Fig. 1 that v_r is very small except for angles near the radial boundaries, and this is clearly the case also for this $c = 0$ wedge. The behavior of v_ϕ with ϕ is also quite similar.

We now return to the technical difficulties with the general solution for the velocity field obtained above via the stream function. As noted in section II A, the quantity $\Psi(r, \phi)$ should be equal to $\Omega r^2/2$ at all points on the boundary, and the physical velocity field should satisfy the boundary conditions $v_\phi(r, \phi) = r\Omega$ for $\phi = 0, \beta$ and $v_r(r, \phi) = 0$ for $r = a$. It is easily seen from Eqs. (2.27) and (2.29b) that both $\Psi(r, \phi)$ and $v_\phi(r, \phi)$ vanish for $\phi = 0$ and $\phi = \beta$ (since $\sin(n\pi\phi/\beta) = 0$ for these values of ϕ). Thus the boundary condition on the radii appears to be violated even though the construction of the vector potential via the Green's function would seem to ensure

that it will not be. As to Eq. (2.29a) for the radial com-

ponent of the velocity, it can be written as

$$v_r(r, \phi) = \frac{8\Omega a^2}{\beta r} \sum_{n \text{ odd}} \cos(n\pi\phi/\beta) \frac{1}{n^2\pi^2/\beta^2 - 4} \left[\left(\frac{r}{a}\right)^{n\pi/\beta} - \frac{r^2}{a^2} \right] - \frac{2\Omega r}{\beta} \sum_{n \text{ odd}} \cos(n\pi\phi/\beta). \quad (2.33)$$

While the first term on the right-hand side of this equation vanishes for $r = a$, the second term does not. Thus, this component also appears not to satisfy the required boundary conditions. Numerically, however, we have found that these quantities do approach values consistent with the required boundary conditions as the boundaries are approached from inside, but there is a discontinuity as the boundary is approached and the values exactly at the boundaries do not satisfy the boundary conditions. This does not affect the calculated values of the angular momentum and the moment of inertia because these quantities are not sensitive to the values of the velocity components exactly at the boundary.

However, this numerical argument is not fully satisfactory. Fortunately there are better ones. First, one can see that this behavior is associated with the nonconvergence of the series. The last term in Eq. (2.33), for example, is not merely nonzero: the series that it contains is not convergent while that in the first term is. Indeed the rearrangement of terms leading from Eq. (2.29a) to Eq. (2.33) isolates just this nonconvergent part. However, by rewriting the cosines in terms of exponentials one can verify that the series in the last term of Eq. (2.33) is Borel summable[20] (and also Euler summable) with the result being zero. With this proviso, Eq. (2.33) satisfies the boundary condition analytically. Similar arguments can be made for Ψ_Ω and for the azimuthal component of the velocity.

This mathematical problem can also be solved by redefining the stream function as

$$\Psi(r, \phi) \rightarrow \Psi(r, \phi) - \frac{2\Omega r^2}{\pi} \left[\sum_{n \text{ odd}} \frac{1}{n} \sin(n\pi\phi/\beta) - \frac{\pi}{4} \right], \quad (2.34)$$

where the first term in the right side is that given by Eq. (2.27). The second term in the right side, which is subtracted from the old expression, is zero for all points inside the wedge [19], and is equal to $-\Omega r^2/2$ for

$\phi = 0, \beta$. Therefore, the subtraction of this quantity does not affect the behavior of $\Psi(r, \phi)$ inside the wedge (where it still satisfies the Laplace equation). At the same time, the redefined $\Psi(r, \phi)$ satisfies the required boundary condition for $\phi = 0, \beta$. The new term leads to the following additional terms in v_ϕ and v_r :

$$v_\phi(r, \phi) \rightarrow v_\phi(r, \phi) - \frac{4\Omega r}{\pi} \left[\sum_{n \text{ odd}} \frac{1}{n} \sin(n\pi\phi/\beta) - \frac{\pi}{4} \right], \quad (2.35)$$

where again the first term in the right side is the previous result, in this case Eq (2.29b). The added quantity is zero at all points inside the wedge, and is equal to Ωr for $\phi = 0, \beta$, so that the required boundary conditions for these values of ϕ are now satisfied. The equation for v_r becomes

$$v_r(r, \phi) \rightarrow v_r(r, \phi) + \frac{2\Omega r}{\beta} \sum_{n \text{ odd}} \cos(n\pi\phi/\beta). \quad (2.36)$$

The new term, added to Eq. (2.29a), cancels the ‘‘offending’’ second term in Eq. (2.33), so that the re-defined v_r satisfies the required boundary condition at $r = a$.

A similar problem with boundary conditions is also present in the solution given in Ref. [1] for the velocity field inside a cylinder with a rectangular cross section. The expression for the stream function given in Eq. (62) of Ref. [1] does not in fact satisfy the required boundary conditions posed there at all points on the boundary. As in the case considered here, this does not affect the results for the calculated physical quantities in Ref. [1], and this mathematical problem can be cured by the addition of a term similar to the one considered above.

The above calculations can be modified readily to treat a superfluid confined in the annular region between two concentric arcs with radii a and b ($a > b$). The Green’s function in this case has the form

$$G(r, \phi; r', \phi') = -\frac{1}{\pi} \sum_{n=1}^{\infty} \frac{1}{n} \frac{1}{1 - (b/a)^{2n\pi/\beta}} \left(r_{<}^{n\pi/\beta} - \frac{b^{2n\pi/\beta}}{r_{<}^{n\pi/\beta}} \right) \times \left(\frac{1}{r_{>}^{n\pi/\beta}} - \frac{r_{>}^{n\pi/\beta}}{a^{2n\pi/\beta}} \right) \sin(n\pi\phi/\beta) \sin(n\pi\phi'/\beta). \quad (2.37)$$

In this case one does not have to worry about the behavior as $r \rightarrow 0$. Asymptotic series in the summations over n are again encountered and handled as in the preceding case. Using this in Eq. (2.23), the stream function $\Psi(r, \phi)$,

and from it, the radial and tangential components of the velocity are obtained. We skip the long expressions for these quantities and quote the final result for the moment of inertia about the origin:

$$I_{SF} = I_{RO} - \frac{16a^4}{\beta} \sum_{n \text{ odd}} \frac{1}{x_n^2(x_n^2 - 4)} \left[\frac{x_n^2 + 4}{2(x_n^2 - 4)}(1 - c^4) - \frac{2x_n}{x_n^2 - 4} \frac{1}{1 - c^{2x_n}} \{(1 + c^4)(1 + c^{2x_n}) - 4c^2 c^{x_n}\} \right]. \quad (2.38)$$

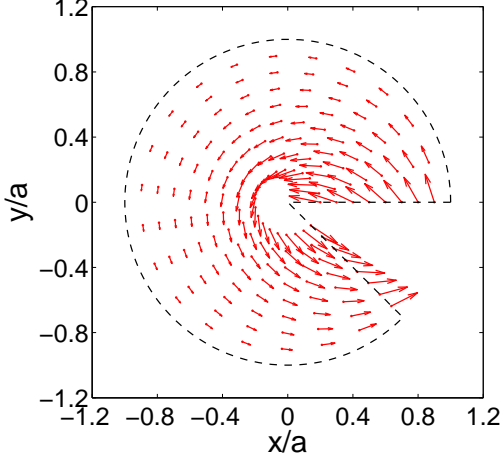


FIG. 4: Plots of the velocity field inside the wedge for $\beta = (7/8)2\pi$. This should be compared with the first panel of Fig. 1.

Here, $x_n = n\pi/\beta$, $c = b/a$, and $I_{RO} = \beta(a^4 - b^4)/4$ is the moment of inertia for rigid-body rotation. We have checked that this expression reduces to that in Eq. (2.30) for $b = 0$, and to that in Eq. (2.22) for $\beta = 2\pi$. In Fig. 5, we show results for the NCRI in an annular wedge, as obtained from Eq. (2.38). The plots are the same as in Fig. 3 except that now we have $c = 0.5$, in other words, the fields are as in Fig. 1. Again, the fractional suppression is larger, as it must be, in the *COM* and it has a maximum at a finite value of β .

D. Formation of vortices in a wedge with $\beta > \pi$

As noted above, the velocity field obtained from a calculation in which it is assumed to be irrotational exhibits a divergence as $r \rightarrow 0$ for a wedge with $\beta > \pi$. Thus v_c must be exceeded near $r = 0$, implying that either there is a region of normal fluid near the tip of the wedge, or a vortex is present in the system. As we have indicated, this issue is unimportant in the torsional oscillation ex-

periments because the region of normal fluid near the tip would be unobservably small for experimentally relevant parameter values. It is, nevertheless, interesting to inquire about the behavior in the general case. We show here that this divergence in the velocity field is eliminated by the introduction of a single vortex.

From symmetry, the vortex must be located along the

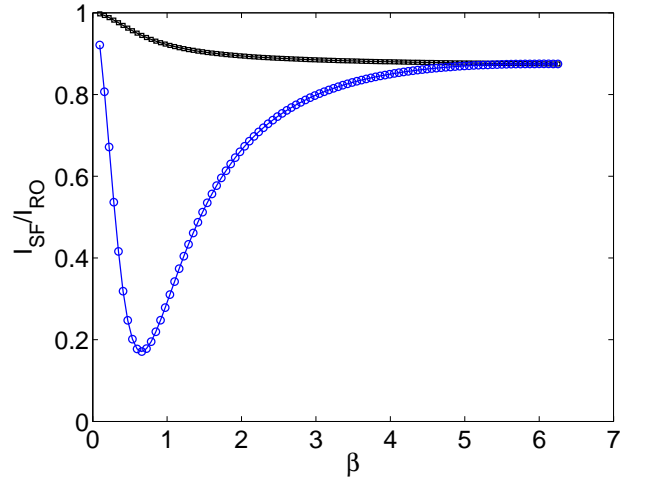


FIG. 5: The ratios I_{SF}/I_{RO} (upper curve), and $I_{SF}^{COM}/I_{RO}^{COM}$ (lower curve) for an annular wedge (Eq. (2.38)) plotted as a function of the opening angle β , $0 < \beta \leq 2\pi$, at a fixed value of $c = 0.5$

line $\phi = \beta/2$. Let the position of the vortex be $(r_v, \beta/2)$. The presence of a vortex of circulation $\kappa (= h/m$, where h is Planck's constant and m is the mass of a particle of the fluid) at (r', ϕ') leads to an additional term, $\kappa G(r, \phi; r', \phi')$ in the expression for the stream function $\Psi(r, \phi)$ where $G(r, \phi; r', \phi')$ is the Green's function given in Eq. (2.26) (see Section 3 of Ref. [1] for a derivation of this result). This additional term in $\Psi(r, \phi)$ (with $r' = r_v, \phi' = \beta/2$) leads to the following additional term in the expression for the radial component of the velocity near $r = 0$:

$$v_r(r, \phi) = v_r^0(r, \phi) + \frac{\kappa}{\beta r} \sum_{n=1}^{\infty} r^{n\pi/\beta} \left(\frac{1}{r_v^{n\pi/\beta}} - \frac{r_v^{n\pi/\beta}}{a^{2n\pi/\beta}} \right) \cos(n\pi\phi/\beta) \sin(n\pi/2) \equiv v_r^0 + v_r^1, \quad (2.39)$$

where $v_r^0(r, \phi)$ is the curl-free result as given by Eqs. (2.36). The $n = 1$ part of the additional term cancels the divergent $n = 1$ contribution of the previous expression if

$$\kappa \left(\frac{1}{r_v^{\pi/\beta}} - \frac{r_v^{\pi/\beta}}{a^{2\pi/\beta}} \right) = 8\Omega a^{2-\pi/\beta} \frac{1}{4 - \pi^2/\beta^2}. \quad (2.40)$$

It is easy to check that the divergence in the expression for the azimuthal component of the velocity is also removed if this condition is satisfied. Defining $(r_v/a)^{\pi/\beta} \equiv \xi$, the solution of Eq. (2.40) is $\xi = [\sqrt{4 + \eta^2} - \eta]/2$, where,

$$\eta \equiv \frac{8\Omega a^2}{\kappa(4 - \pi^2/\beta^2)} > 0. \quad (2.41)$$

One sees that ξ has the nice property that $0 < \xi < 1$ for any value of η . The value of ξ changes from 1 to 0 as the dimensionless parameter $\gamma \equiv \Omega a^2/\kappa$ increases from zero to a large value, i.e. the vortex moves inward from the rim of the wedge to its tip as the angular velocity increases.

Using the expressions for the radial and tangential components of the velocity in the presence of a vortex, the total angular momentum of the superfluid can be calculated. The presence of the vortex increases the angular momentum about the origin by the amount L_v and the moment of inertia for rotation about the origin by $I_V = L_V/\Omega$. Using the result for the vortex position, this can be written as

$$I_V = \frac{64a^4}{\pi} \frac{1}{[4 - \pi^2/\beta^2][(a/r_v)^{\pi/\beta} - (r_v/a)^{\pi/\beta}]} \times \sum_{n \text{ odd}} (-1)^{\frac{n+1}{2}} \frac{1}{n(4 - n^2\pi^2/\beta^2)} \left[\left(\frac{r_v}{a} \right)^2 - \left(\frac{r_v}{a} \right)^{n\pi/\beta} \right]. \quad (2.42)$$

In the presence of the vortex, the moment of inertia about the origin is $(I_{SF} + I_V)$ where I_{SF} is given by Eq. (2.30) and I_V is given by the equation above. The value of r_v/a to be used in this equation is given by the solution of Eq. (2.40). Since the vortex position r_v depends on the angular speed Ω , the value of I_V also depends on Ω .

Although the divergence in the velocity field at small r is eliminated by the introduction of a vortex, the free energy of the state with this vortex is not necessarily lower than that of the vortex-free state with a small region of normal fluid near $r = 0$. Specifically, in the experimental situations discussed above where the dimensions of the region of normal fluid are extremely small, the free energy cost of creating the normal region is negligible and the free energy cost of creating a vortex is the deciding factor in determining whether a vortex will be present. We therefore calculate, in the following subsection, the free energy of a state with a single vortex.

E. Free energy of a vortex and critical angular velocity for vortex nucleation

In the free energy calculation, we consider the general case of a ring with $b \neq 0$. The angular speed Ω_1 at which nucleation of a first vortex will occur can be determined from free energy considerations. The free energy F is

given[1] in terms of the energy E and the angular momentum L as:

$$F = E - L\Omega \quad (2.43)$$

We will denote here with a subscript 0 the quantities F , E and L in the vortex-free state, and with a 1 subscript those in the presence of one vortex. As stated in the preceding subsection, the stream function in the presence of a vortex is:

$$\Psi_1(\mathbf{r}) = \Psi_0(\mathbf{r}) + \kappa G(\mathbf{r}, \mathbf{r}') \equiv \Psi_0 + \Psi_1 \quad (2.44)$$

where $G(\mathbf{r}, \mathbf{r}')$ is the Green's function given in Eq. (2.37) and \mathbf{r}' is the vortex position with coordinates r', ϕ' . From symmetry considerations $\phi' = \beta/2$ and the equilibrium radial position of the vortex, $r' = r_v$, is to be determined from free energy minimization. The velocity field and the angular momentum in the presence of a vortex can be readily obtained from the stream function of Eq. (2.44). The angular momentum is given by

$$L_1 = L_0 + \kappa a^2 C \quad (2.45)$$

where the dimensionless quantity C has the following expression:

$$C = \frac{8}{\pi} \sum_{n \text{ odd}} (-1)^{\frac{n+1}{2}} \frac{1}{n} \frac{1}{4 - x_n^2} \frac{1}{1 - c^{2x_n}} \times [(r'/a)^2(1 - c^{2x_n}) - (r'/a)^{x_n}(1 - c^{x_n+2}) - (ca/r')^{x_n}(c^2 - c^{x_n})], \quad (2.46)$$

with $x_n = n\pi/\beta$.

It is not hard to see explicitly that $G(\mathbf{r}, \mathbf{r}')$ has, as expected, a logarithmic singularity at \mathbf{r}' , so that we can write:

$$G(\mathbf{r}, \mathbf{r}') = \frac{1}{2\pi} \ln(|\mathbf{r} - \mathbf{r}'|/\alpha) + g(\mathbf{r}, \mathbf{r}') \quad (2.47)$$

where α is the radius of the vortex core and $g(\mathbf{r}, \mathbf{r}')$, the nonsingular part of the Green's function, satisfies the Laplace equation. As shown in Ref. [1] (see also Ref. [21]), the energy in the presence of a vortex can be written as

$$E_1 = \frac{1}{2}L_1\Omega + \frac{1}{4}\kappa\Omega r'^2 - \frac{1}{2}\kappa\Psi_0(\mathbf{r}') - \frac{1}{2}\kappa^2g(\mathbf{r}', \mathbf{r}'). \quad (2.48)$$

After some algebra, the nonsingular part of the Green's function appearing in Eq.(2.48) is obtained as

$$g(\mathbf{r}', \mathbf{r}') = \frac{1}{2\pi} \ln\left(\frac{\pi\alpha}{2\beta r'}\right) - \frac{1}{\pi} \sum_{n \text{ odd}} \frac{1}{n} \frac{1}{1 - c^{2x_n}} [2c^{2x_n} - (r'/a)^{2x_n} - (ca/r')^{2x_n}], \quad (2.49)$$

where $x_n = n\pi/\beta$. Using Eqs. (2.45), (2.46), (2.48) and (2.49), the free energy in the presence of a vortex at $(r', \beta/2)$ may be obtained. The results depend on the vortex core size, via the logarithmic dependence on a/α mentioned above. One then minimizes F_1 with respect to r' to obtain its optimal value r_v , and compares F_1 and F_0 to find the overall equilibrium state. This depends on the value of Ω and, for sufficiently small Ω , it is the vortex-free state, while for $\Omega > \Omega_1$ the one-vortex state first becomes favorable. In practice these calculations can be done only numerically, but the computations are not difficult. The relevant dimensionless parameter is the quantity $\gamma = \Omega a^2/\kappa$ defined in the preceding section. This parameter is the ratio of the characteristic scale, Ωa , of the velocity field \mathbf{v}^0 due to the rotation alone, and the scale of the additional velocity field \mathbf{v}^1 due to the vortex, which is κ/a . One needs also to input the value of α/a for which we take the physically reasonable value of 10^7 .

Results for Ω_1 computed for a blocked annular ring ($\beta = 2\pi$) are given in Fig. 6. There we plot the critical value of γ vs the aspect ratio c . We see that at reasonably small or intermediate values of c the critical value of γ is in the range 10-50 corresponding to angular speeds in the general range of $10^{-1}/s$, which is in the experimentally relevant region. At large values of c this quantity increases, reflecting that the system is behaving more like a rigid body, in which case the formation of vortices is obviously less favorable. A similar trend was seen for progressively flatter ellipsoids in Ref. 1. This implies that the conclusions reached in our calculations without vortices about the sharp discontinuities that should occur when a reasonably narrow ring is obstructed or unobstructed are valid in the experimentally interesting range.

In Fig. 7, we show the texture of the velocity field \mathbf{v}^1 due to the nucleated vortex alone at $c = 0.5$ and at a value of γ slightly higher than its critical value, which at this value of c is $\gamma_1 \simeq 20$ (see Fig. 6). The calculated optimal position of the vortex at these values of γ and c is $r_v/a = 0.74$. This position is marked by a (blue) circle in the plot. The fields in this figure should be combined with those in the top panel of Fig. 1. One should recall that

both plots are in arbitrary units, so that before plotting the combined field one should divide the fields in Fig. 7 by $\gamma \simeq 20$ to take into account their overall smaller relative scale. If that were done, however, then the plot would be very hard to distinguish with the naked eye from that in the top panel of Fig. 1. For this reason, in order to give the reader a clearer feeling for the overall texture of the combined fields, we have plotted them in Fig. 8 after multiplying the \mathbf{v}^1 by a relative weight of $1/2$, rather than $1/20$.

The moment of inertia of a ring in the presence of a nucleated vortex may be calculated from Eqs. (2.45) and (2.46). The results deviate from those obtained for the vortex-free state only by a correction of order $1/\gamma$. For $\Omega \geq \Omega_1$ this is therefore significant only at small values of c . At $c \rightarrow 0$ we find for example that, at $\beta = 2\pi$, the

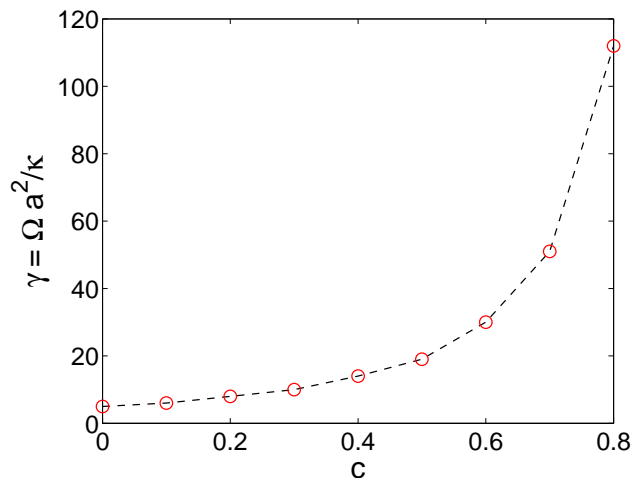


FIG. 6: The critical angular velocity for vortex nucleation in a ring ($\beta = 2\pi$). Here the critical value of the parameter γ (i.e. $\Omega_1 a^2/\kappa$) is plotted as a function of c . The circles are numerical results, connected by straight dashed lines. The increase at larger c shows that the nucleation of vortices is unfavorable in that case.

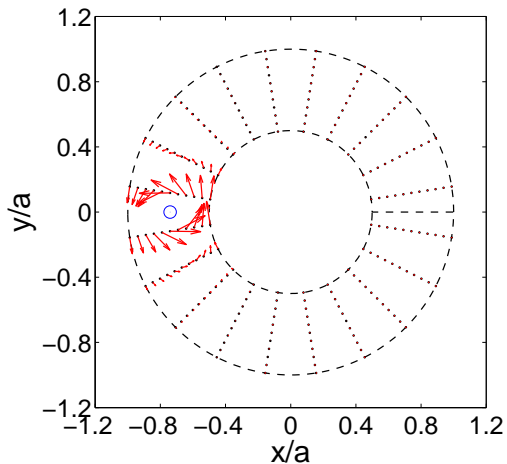


FIG. 7: (Color online) Fields produced by a nucleated vortex in an obstructed ring with $c = 0.5$, at $\Omega = \Omega_1$. Only the fields produced by the vortex are included. Its position (marked by a (blue) open dot) is at the optimal value (see text) $r_v/a = 0.74$. The total flow is the sum of that shown in this figure, weighed by a factor of $1/\gamma$, and that in the top panel of Fig. 1. Because γ is rather large, the result would be hard to distinguish from that shown in Fig. 1.

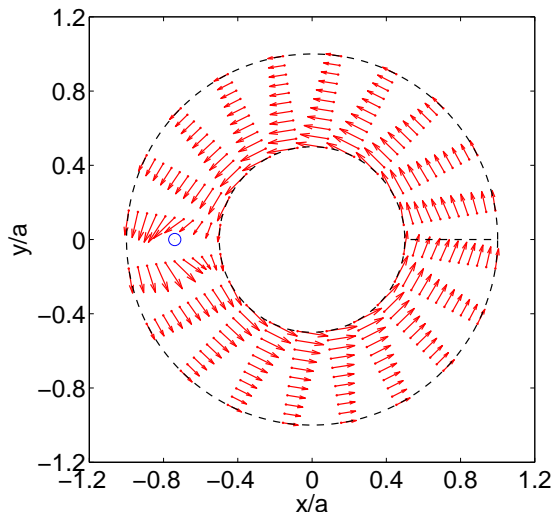


FIG. 8: (Color online) Combined velocity fields in the presence of a vortex. This is the weighted sum of the fields in the top panel in Fig. 1 and those in Fig. 7. As discussed in the text, the effect of the vortex has been artificially enhanced for visibility purposes by using a weight factor of $1/2$ for the vortex fields, rather than the actual $1/20$.

moment of inertia of a blocked wedge ($c = 0$) increases by about 8.3% as a vortex is nucleated at $\Omega = \Omega_1$, and the increase in the moment of inertia due to the nucleation of a vortex becomes less than 1% for $c \geq 0.33$.

The optimal value, r_v , of the radial coordinate of the vortex obtained from free-energy minimization is quite

different from the value for which the velocity due to the vortex cancels the mathematical singularity at $r = 0$ found in wedges with $\beta > \pi$. This implies that the velocity field would formally diverge at $r = 0$ in such systems even when a vortex is present at the position corresponding to the minimum of the free energy. As noted above, this mathematical singularity does not have any physical consequence in the usual experimentally studied situations. This interplay between the requirements of keeping the velocity below the Landau critical value and minimizing the free energy may lead to interesting behavior in other possible experimentally accessible situations.

III. SUMMARY AND DISCUSSION

We have calculated here the velocity fields of a superfluid sample in a cylindrical wedge, or ring-wedge geometry. We have used two different methods to solve the relevant hydrodynamic equations both in the absence of vortices and when vortices are present. From the resulting velocity fields, we have derived formulas for the moment of inertia, and therefore for the NCRI effect in these geometries.

Physically, the most important of our results is that the NCRI effect is most prominent for relatively narrow rings. Our calculations show that the moment of inertia of a blocked narrow ring is very close to the rigid-body value unless the width of the ring is a large fraction of its outer radius. Since the moment of inertia of a superfluid ring for rotation about its center is zero when it is unblocked (at least for small Ω), one should see a considerable change in the NCRI when approximately circular superfluid channels in a sample are obstructed or unobstructed. The fractional change in the moment of inertia as a ring is unblocked (defined relative to the moment of inertia of the ring for rigid-body rotation) is maximum when the rotation axis passes through the center of the ring. In that case, this ratio approaches unity very quickly as the aspect ratio c of the ring is increased toward one (see Fig. 2, top panel), and this ratio has a value close to 0.44 as $c \rightarrow 0$. The magnitude of the change in the rotational inertia upon blocking/unblocking does not depend on the location of the axis of rotation. For a fixed value of the outer radius a , the magnitude of this change is maximum when the aspect ratio c is close to 0.52 (see Fig. 2, bottom panel). This maximum is very broad. For an annular superfluid wedge, the moment of inertia about an axis passing through its tip is close to the rigid-body value if the opening angle β is small, and it decreases as β is increased (see Figs. 3 and 5).

The results summarized above are for the case where there are no vortices, so that the velocity field is irrotational. Since one expects vortices to be nucleated as the rotational speed is increased, we have used a free-energy criterion to determine the critical angular speed for the nucleation of a vortex in the system. We find that the experimentally relevant range of geometries and

speeds includes both the parameter region where vortices are absent and that where nucleated vortices exist. For a fixed value of $\beta = 2\pi$ (ring geometry), the critical angular speed increases rapidly as the aspect ratio c is increased above about 0.5 (see Fig. 6). Also, the increase in the moment of inertia due to the nucleation of a vortex is rather small (less than 10%) in all cases. These observations imply that the results mentioned above for a narrow ring without vortices remain valid for relatively large values of the angular velocity.

Mathematically, a number of relevant results have been uncovered and emphasized. There are a number of technical difficulties in the calculation of the velocity fields, leading to non-convergent series and singularities. However, the singularities are integrable and the series are Borel summable, so that there is no difficulty in calculating physical quantities such as the angular momentum and the kinetic energy. We also point out the occurrence of a mathematical singularity in the velocity field

in wedges (but not in rings) with $\beta > \pi$ and discuss briefly possible effects of this divergence. This singularity turns out to have no measurable consequence in commonly studied experimental situations.

In general, the ideas and methods developed here can be used in other geometries. We believe that the results and techniques presented here can be very useful in understanding not only NCRI phenomena in “supersolid” helium, but also superflow in confined geometries and in finite systems. Work in which we apply these ideas to study the NCRI effect in realistic models of grain boundary networks is in progress.

Acknowledgments

This work was supported in part by NSF (OISE-0352598) and by DST (India).

-
- [1] A. L. Fetter, *J. Low Temp. Phys.* **16**, 533 (1974).
 [2] E. Kim and M.W.H. Chan, *Science* **305**, 1941 (2004).
 [3] E. Kim and M.W.H. Chan, *Phys. Rev. Lett.* **97**, 115302 (2006).
 [4] A. C. Clark, J.T. West and M.W.H. Chan, *Phys. Rev. Lett.* **99**, 135302 (2007).
 [5] A.S.C. Rittner and J.D. Reppy, *Phys. Rev. Lett.* **97**, 165301 (2006); *ibid.* **98**, 175302 (2007).
 [6] Y. Aoki, J.C. Graves and H. Kojima, *Phys. Rev. Lett.* **99**, 015301 (2007).
 [7] S. Sasaki, R. Ishiguro, F. Caupin, H.J. Maris and S. Balibar, *Science* **313**, 1098 (2006).
 [8] L. Pollet, M. Boninsegni, A.B. Kuklov, N.V. Prokof'ev, B.V. Svistunov and M. Troyer, *Phys. Rev. Lett.* **98**, 135301 (2007).
 [9] R. Onofrio, C. Raman, J.M. Vogels, J.R. Abo-Shaeer, A.P. Chikkatur and W. Ketterle, *Phys. Rev. Lett.* **85**, 2228 (2000).
 [10] O.M. Marago, S.A. Hopkins, J. Arlt, E. Hodby, G. Hechenblaikner, and C. J. Foot, *Phys. Rev. Lett.* **84**, 2056 (2000).
 [11] C. Ryu, M.F. Andersen, P. Clade, V. Natarajan, K. Helmerson and W.D. Phillips, *Phys. Rev. Lett.* **99**, 260401 (2007).
 [12] B. Clancey, L. Luo and J.E. Thomas, *Phys. Rev. Lett.* **99**, 140401 (2007).
 [13] L. Amico, A. Osterloh and F. Cataliotti, *Phys. Rev. Lett.* **95**, 063201 (2005).
 [14] J.B. Mehl and W. Zimmermann, Jr., *Phys. Rev.* **167**, 214 (1968).
 [15] L.-z. Cao, D.F. Brewer, C. Girit, E.N. Smith and J.D. Reppy, *Phys. Rev. B* **33**, 106 (1986).
 [16] E. Kim and M.W.H. Chan, *Nature* **427**, 225 (2004).
 [17] See e.g. Ch. 13 in K. Huang, *Statistical Mechanics*, Wiley, New York, (1987).
 [18] See page 142 in J. D. Jackson, *Classical Electrodynamics*, 3rd Edition, Wiley, New York (1999).
 [19] See page 38 in I.S. Gradshteyn and I.M. Ryzhik, *Table of Integrals, Series and Products*, Academic Press, New York, (1980).
 [20] See Chapter 8 in C.M. Bender and S.A. Orszag, *Advanced Mathematical Methods for Scientists and Engineers*, Springer Verlag, New York (1991).
 [21] A.L. Fetter, *Phys. Rev.* **152**, 183 (1966).